Science Advances Today

Sci. Adv. Today 2 (2016) 25239

ISSN 2455-2321

Synthesis, spectroscopic investigations, quantum chemical studies, molecular docking and antiviral activity of 5-chloro-N-(2-chlorophenyl)pyrazine-2-carboxamide

S. H. Rosline Sebastian[a,b], Monirah A. Al-Alshaikh[c], Ali A. El-Emam[d], Sheena Mary Y[e], C. Yohannan Panicker[e,*], P. J. Jojo[e], Jan Zitko[f], Martin Dolesal[f]

[a] Department of Physics, Karpagam University, Eachanari, Coimbatore, Tamilnadu, India
[b] Christhu Jyothi Public School, Rajakkad, Idukki, Kerala, India
[c] Department of Chemistry, College of Sciences, King Saud University, Riyadh 11451, Saudi Arabia
[d] Department of Pharmaceutical Chemistry, College of Pharmacy, King Saud University, Riyadh 11451, Saudi Arabia
[e] Department of Physics, Fatima Mata National College, Kollam, Kerala, India
[f] Faculty of Pharmacy in Hradec Kralove, Charles University in Prague, Heyrovskeho 1203, Hradec Kralove 500 05, Czech Republic

[*]Author for correspondence: C. Yohannan Panicker, email: cyphyp@rediffmail.com
Received 05 Mar 2016, Accepted 26 Apr 2016, Published Online 26 Apr 2016

The FT-IR and FT-Raman spectra of 5-chloro-N-(2-chlorophenyl)pyrazine-2-carboxamide were recorded and the vibrational wavenumbers are computed using DFT method. On the basis of potential energy distribution the complete vibrational assignments were performed. From the molecular electrostatic potential study the negative potential regions are mainly localized over the carbonyl group and phenyl ring and are possible sites for electrophilic attack. The calculated HOMO and LUMO energies confirm that charge transfer occurs within the molecule. The geometrical parameters of the title compound are in agreement with that of similar compounds. The calculated first hyperpolarizability value is comparabel with that of similar derivatives and the study of second hyperpolarizability reveals that the title compound is an attractive object for future studies in nonlinear optics. From the molecular docking study, the docked ligand title compound forms a stable complex with glucosamine 6-phosphate deaminase from *E.coli* and gives a binding affinity value of -6.4kcal/mol. The results suggest that the compound might exhibit inhibitory activity against glucosamine 6-phosphate deaminase. The title compound was tested for *in vitro* activity against various DNA and RNA viruses, but no activity was observed.

1. INTRODUCTION

Pyarzines occur almost ubiquitously in nature and obtained from fused oil, galbanum oil, cocoa butter, cocoa bean, coffe bean, green peas, mandibular gland secretion of ponecine ants, molds like *Aspergillus (A) flacus, A.sclerotioriu, A.oryazae, A.ochraceus* etc [1]. The beauty of pyrazine derivatives is that ring carbon atoms can be substituted to get different derivatives [2]. Pyrazines are found naturally in many vegetables, insects, terrestrial vertebrates, and marine organisms, and they are produced by microorganisms during their primary or secondary metabolism [3-6]. The widespread occurrence of simple pyrazine molecules in nature, especially in the flavours of many food systems, their effectiveness at very low concentrations as well as the still increasing applications of synthetic pyrazines in the flavor and fragrance industry are responsible for the high interest in these compounds [7]. Certain pyrazines, especially dihydropyrazines, are essential for all forms of life due their DNA strand-breakage activity and/ or by their influencing of apoptosis [8]. Pyrazinamide (pyrazine-2-carboxamide) is a first-line antitubercular drug and pyrazinamide derivatives are still in the focus of antitubercular research. The title compound of this article, 5-chloro-*N*-(2-chlorophenyl)pyrazine-2-carboxamide, possessed *in vitro* anti mycobaterial activity against *M. tuberculosis* H37Rv with minimum inhibitory concentration of 0.78-3.13 µg/mL [9]. Certain pyrazine carboxamide derivatives were found to show good inhibitory activity against influenza viruses [10, 11], bovine virus diarrhea [12], yellow fever [13-15] and Puna Toro virus [16]. Therefore, based on the presence of the pyrazine-2-carboxamide moiety, the title compound 5-chloro-*N*-(2-chlorophenyl)pyrazine-2-carboxamide was tested for *in vitro* activity against a broad panel of viruses, including those mentioned above.

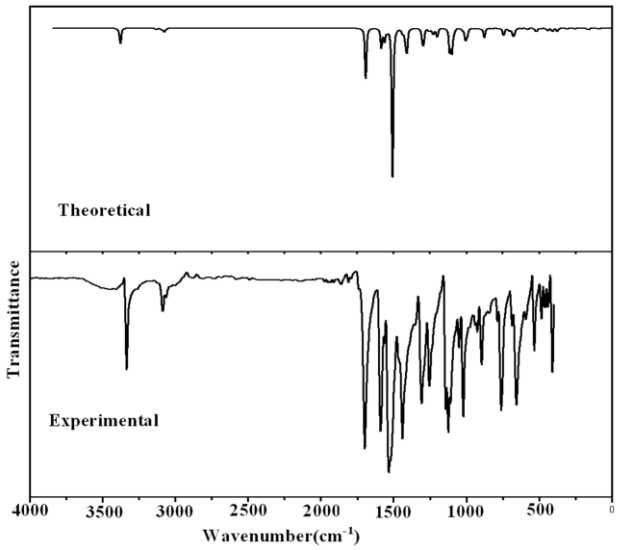

Figure 1. FT-IR spectrum of 5-chloro-N-(2-chlorophenyl) pyrazine-2-carboxamide.

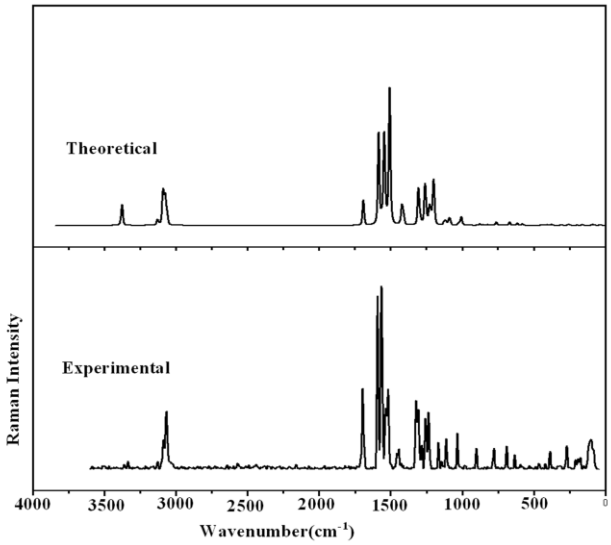

Figure 2. FT-Raman spectrum of 5-chloro-N-(2-chlorophenyl) pyrazine-2-carboxamide.

2. MATERIALS AND METHODS

2.1. General

The sample of the title compound was obtained from the authors of previous study of this compound [9]. The identity and purity of the sample was checked by melting point, NMR spectra and TLC analysis. Obtained results were fully consistent with those reported in literature [17]. The FT-IR spectrum (Figure 1) was recorded using KBr pellets on DR/Jasco FT-IR spectrometer and the FT-Raman spectrum (Figure 2) was obtained on a Bruker RFS 100/s, Germany.

2.2. Antiviral Evaluation

Antiviral activity in cell culture was assessed by cytopathic effect (CPE) reduction assays. To perform the tests, the virus was added to semiconfluent cell cultures in 96-well plates and, simultaneously, serial dilutions of the test compound were added. The plates were incubated untile clear CPE was reached (typically 3-6 days). The antiviral activity was expressed as EC_{50}, which is the effective concentration causing 50% reduction of CPE compared no non-treated infected cells. The CPE was evaluated by visual microscopy and/or by standard colorimetric formazan-based MTS cell viability assay. Viruses examined in Crandell-Rees Feline Kidney (CRFK) cells: feline coronal virus; feline herpes virus. Viruses examined in human embryonic lung fibroblast (HEL) cells: herpes simplex virus type 1 (HSV-1); a thymidine kinase-deficient (TK) HSV-1 KOS strain resistant to aciclovir; herpes simplex virus type 2 (HSV-2); vaccinia virus; human adenovirus type 2; and vesicular stomatitis virus (VSV). Viruses examined in human cervix carcinoma (HeLa) cells: VSV; Coxsackie B4 viurs; and respiratory syncytial virus (RSV). Viruses examined in African Green Monkey (Vero) cells: para-influenza-3 virus; reovirus-1; Sindbis virus; Coxsackie B4 virus and Punta Toro virus. Viruses examined in Madin-Darby canne kidney (MDCK) cells: human influenza A/H1N1, A/H3N2 and B viruses. Finally, activity against human immunodefiency virus (HIV) type 1 and type 2 was studied in human MT-4 lymphoblast cells.

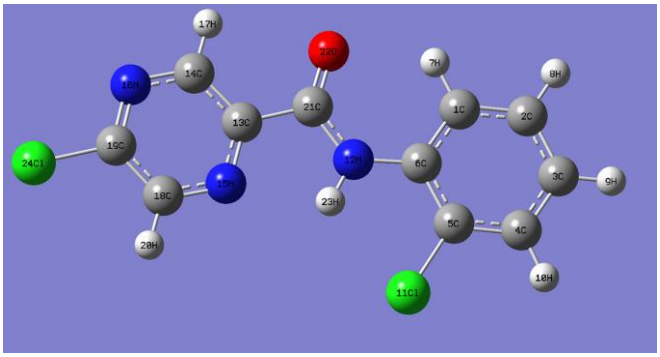

Figure 3. Optimized geometry of 5-chloro-N-(2-chlorophenyl) pyrazine-2-carboxamide.

2.3. Computational Details

Gaussian09 [18] software was used for all the theoretical calculations and structure of the title compound was optimized using the Becke-Lee-Yang-Parr hybrid exchange correlation three-parameter functional (B3LYP) with CC-pVDZ (5D, 7F) basis set [19]. A scaling factor of 0.9613 had to be used for obtaining a considerably better agreement with experimental data [20]. Structural parameters corresponding to the optimzied geometry of the title compound (Figure 3) are given in Table 1. The assignments of the calculated frequencies are done using Gaussview [21] and GAR2PED [22] software.

3. RESULTS AND DISCUSSION

3.1. Geometrical Parameters

In the folowing discussion, the phenyl and pyrazine ring are designated as Ph and Pz, respectively. The C-C bond lengths in the phenyl ring lie in the range 1.3927-1.4117Å and for benzene the C-C bond length is 1.3993Å [23] and for benzaldehyde 1.3973Å [24]. In the present case, the bond lengths, C_{13}-C_{21} =1.5084, C_{21}-O_{22} =1.2256, C_{21}-N_{12} = 1.3685, C_6-N_{12} = 1.4006Å are and the correspondng reported values are 1.5248, 1.2486, 1.3521, 1.4109Å [25]. For the title compound, the pyrazine bond lengths, C_{13}-C_{14} = 1.3992, C_{14}-N_{16} = 1.3402, C_{19}-N_{16} =1.3221, C_{19}-C_{18} =1.4055, C_{18}-N_{15} =1.3300 and C_{13}-N_{15} = 1.3437Å and the corressponding reported values are 1.3955, 1.3482, 1.3521, 1.4109, 1.3532, 1.3477Å [25]. The C-N bond lengths in the pyrazine ring of the title compound are much shorter than the normal C-N sing bond that is referred to 1.49Å [25] and the same results are shown for the two C-C bonds lengths in the pyrazine ring and are also smaller than that of the normal C-C single bond of 1.54Å [26]. The bond lengths C_{21}-N_{12} = 1.3685 and C_6-N_{12} = 1.4006Å are also shorter than the normal C-N single bond of 1.49Å, which confirms this bond to have some character of a double or conjugated bond [27]. For the

Table 1. Optimized geometrical parameters of 5-chloro-N-(2-chlorophenyl)pyrazine-2-carboxamide.

Bond lengths (Å)

C1-C2	1.3948	C1-C6	1.4082	C1-H7	1.0870
C2-C3	1.3968	C2-H8	1.0919	C3-C4	1.3964
C3-H9	1.0914	C4-C5	1.3927	C4-H10	1.0903
C5-C6	1.4117	C5-Cl11	1.7670	C6-N12	1.4006
N12-C21	1.3685	N12-H23	1.0194	C13-C14	1.3992
C13-N15	1.3437	C13-C21	1.5084	C14-N16	1.3402
C14-H17	1.0914	N15-C18	1.3300	N16-C19	1.3221
C18-C19	1.4055	C18-H20	1.0922	C19-Cl24	1.7524
C21-O22	1.2256				

Bond angles (˚)

C2-C1-H7	121.3	C6-C1-H7	118.3
C2-C1-C6	120.4	C3-C2-H8	120.1
C1-C2-C3	121.0	C1-C2-H8	118.9
C2-C3-C4	119.5	C2-C3-H9	120.8
C4-C3-H9	119.8	C3-C4-C5	119.7
C3-C4-H10	121.2	C5-C4-H10	119.2
C4-C5-C6	121.7	C4-C5-Cl11	118.6
C6-C5-Cl11	119.7	C1-C6-N12	123.2
C1-C6-C5	117.8	C5-C6-N12	119.0
C6-N12-C21	128.6	C6-N12-H23	116.8
C21-N12-H23	114.6	C14-C13-N15	121.3
C14-C13-C21	119.6	N15-C13-C21	119.1
C13-C14-N16	121.7	C13-C14-H17	120.3
N16-C14-H17	118.0	C13-N15-C18	117.4
C14-N16-C19	116.1	N15-C18-C19	120.2
N15-C18-H20	118.4	C19-C18-H20	121.4
N16-C19-C18	123.3	N16-C19-Cl24	117.9
C18-C19-Cl24	118.9	N12-C21-C13	112.9
N12-C21-O22	126.5	C13-C21-O22	120.7

title compound C=O bond length is 1.2256Å and the corresponding reported values are 1.2253Å [28], 1.2486Å [25] and 1.2253Å [29] and according to literature [30, 31] the changes in bond lengths in C=O and C-N are consistent with the following interpretation: that is, hydrogen bond decreases the double bond character of C=O bond and increases the double bond character of C-N bond. At N_{12} position, the angles C_6-N_{12}-H_{23} is 116.8˚, C_{21}-N_{12}-H_{23} is 114.6˚ and C_6-N_{12}-C_{21} is 128.6˚ and this asymmetry of angles at N_{12} position indicates the weakening of N_{12}-H_{23} bond resulting in proton transfer to the oxygen atom O_{22} [32]. At C_{13} position the angles C_{14}-C_{13}-N_{15} is increased by 1.3˚ and N_{15}-C_{13}-C_{21} is reduced by 0.9˚ from 120˚ and this asymmetry reveals the interaction between the amide moiety and the pyrazine ring. At C_{21} position, the bond angles are C_{13}-C_{21}-N_{12} =112.9˚, C_{13}-C_{21}-O_{22} = 120.7˚ and N_{12}-C_{21}-O_{22} = 126.5˚ and this asymmetry gives the interaction between carbonyl group and the neighbouring pyrazine ring.

3.2. IR and Raman spectra

The observed IR, Raman bands, calculated (scaled wavenumbers) and assignments are given in Table 2. For the title compound, the C-Cl stretching mode is assigned at 664 cm^{-1} in the IR spectrum and at 703, 668 cm^{-1} theoretically as expected [33, 34]. The C-Cl stretching modes ares reported at 671 cm^{-1} [35], 660 (IR), 666 (Raman), 670, 657 cm^{-1} (DFT) [36]. For the title compound the C=O stretching mode is observed at 1698 cm^{-1} in the IR spectrum and at 1696 cm^{-1} in the Raman spectrum. The corresponding theoretical value is 1691 cm^{-1} and according to literature, C=O stretching modes are expected in the range 1715-1600 cm^{-1} [37, 38]. The NH stretching mode of the title compound is assigned at 3350 (IR), 3345 (Raman) and 3378 cm^{-1} (DFT) which is expected in the region 3390 ± 60 cm^{-1} [37]. In the present case, the NH deformations are assigned at 1507, 1210 cm^{-1} (DFT) and the reported values are 1500, 1239 (IR), 1497, 1248 cm^{-1} (DFT) [25]. The out-of-plane NH deformation mode is assigned at 681 cm^{-1} in the IR spectrum, 683 cm^{-1} in the Raman spectrum and at 679 cm^{-1} theroeitcally which is expected in the region 790 ± 70 cm^{-1} [37]. The C-N stretching mode coupled with NH deformation is active in the region 1275 ± 55 cm^{-1} [37, 38] and in the present case bands at 1230 (Raman), 1227, 1210 cm^{-1} (DFT) are assigned as the CN stretching modes. The reported values are 1265, 1239 (IR) and 1261, 1248 cm^{-1} (DFT) for a similar derivative [25]. Mary et al. [39] reported the NH modes at 1547, 1250, 650 (IR) and 1580, 1227, 652 cm^{-1} (theoretically) for a similar derivative.

The pyrazine ring streching modes are assigned at 1542, 1520, 1307, 1200, 1084 cm^{-1} in the IR spectrum, 1542, 1309 cm^{-1} in the Raman spectrum and in the range 1544-1088 cm^{-1} theoretically for the title compound. The reported values of the pyrazine ring stretching modes are 1527, 1481, 1219, 1207, 1177 cm^{-1} [40], 1550, 1518, 1193, 1152, 1045 cm^{-1} [25]. The ring breathing mode of the pyrazine ring is assigned at 1115 cm^{-1} theoretically for the title compound and the ring breathing mode is reported at 1126 cm^{-1} [40] and at 1131 cm^{-1} [41]. The CH modes of the pyrazine ring are assinged at 3088, 3071, (DFT), 3071 cm^{-1} (Raman) (stretching modes), 1230 (Raman), 1251, 1227 cm^{-1} (DFT) (in-plane deformation) and 943, 896 (IR), 901 (Raman), 945, 898 cm^{-1} (DFT)

Table 2. Calculated (scaled) wavenumbers, observed IR, Raman bands and assignments of 5-chloro-N-(2-chlorophenyl)pyrazine-2-carboxamide.

B3LYP) with CC-pVDZ (5D, 7F)			IR $\upsilon(cm^{-1})$	Raman $\upsilon(cm^{-1})$	Assignments[a]
$\upsilon(cm^{-1})$	IR_I	R_A			
3378	77.68	217.34	3350	3345	υNH(99)
3128	8.20	56.13	3125	3130	υCHPh(98)
3091	6.26	225.73	3091	3090	υCHPh(96)
3088	0.73	83.26	-	-	υCHPz(99)
3077	11.95	182.20	-	-	υCHPh(98)
3071	6.06	90.07	-	3071	υCHPz(99)
3063	2.69	77.50	3063	-	υCHPh(95)
1691	223.61	146.38	1698	1696	υC=O(80)
1584	83.62	513.38	1588	1588	υPh(61), δPh(10)
1563	62.71	38.21	1564	1565	υPh(59)
1544	13.99	554.63	1542	1542	υPz(63), δCHPz(15)
1518	9.57	68.24	1520	-	υPz(77)
1507	654.47	731.04	-	1510	δNH(51), υPh(10)
1438	19.77	6.85	1440	1440	υPh(44), δCHPh(34)
1420	42.27	139.51	-	-	δCHPz(15), υPz(51)
1410	133.07	43.25	-	-	δCHPh(30), υPh(24), δCHPz(12)
1306	13.36	192.30	1307	1309	υPz(41), υPh(23)
1296	111.57	52.06	-	1293	υPh(59)
1260	6.36	208.92	1261	1260	δCHPh(47), υCN(41)
1251	12.07	51.91	-	-	δCHPz(43), υPz(26), υCC(11)
1227	37.40	138.53	-	1230	δCHPz(46), υCN(39)
1210	3.10	40.79	-	-	δNH(47), υCN(38)
1200	36.05	222.91	1200	-	υPz(51), δCHPz(10)
1127	1.00	26.33	-	-	δCHPh(85)
1115	99.14	18.28	1118	1114	υCN(19), υPz(50)
1100	101.92	6.00	1104	-	δCHPh(19), υPz(16), υPh(22)
1088	30.73	53.09	1084	-	υCN(13), υPz(57)
1026	5.74	15.62	1024	1030	υPh(46), δCHPh(23), δPh(12)
1009	46.08	42.99	-	-	δCHPh(49), υCCl(17), υPh(20)
996	49.34	6.53	-	993	δPz(57), υPz(24)
970	0.63	0.45	972	-	γCHPh(82), τPh(12)
945	1.73	1.86	943	-	γCHPz(80), τPh(10)
929	2.15	0.18	926	-	γCHPh(89)
898	5.29	0.45	896	901	γCHPz(81)
876	42.58	8.60	-	-	δNH(23), δC=O(28)
855	0.92	3.56	853	850	γCHPh(78)
822	2.66	4.83	-	-	δPh(37), υCN(15), υPh(13)
780	1.84	2.89	782	782	τPz(53), γCC(19), γC=O(14)
761	0.76	15.24	760	-	δPz(40), υCCl(13)
743	42.79	1.51	-	-	γCHPh(91)
709	4.46	1.96	-	-	τPh(54), γCN(15), γCCl(12)
703	11.15	0.32	-	-	τPh(15), τPz(19), υCCl(40)
679	40.85	2.73	681	683	γC=O(30), γNH(36), τPz(19)
668	15.92	14.97	664	-	δPh(27), υCCl(46)
617	1.15	13.57	-	-	δPz(77)
579	5.61	9.73	-	-	δPh(68)
536	0.30	0.21	535	533	τPh(56), γCN(21)

Table 2. Calculated (scaled) wavenumbers, observed IR, Raman bands and assignments of 5-chloro-N-(2-chlorophenyl)pyrazine-2-carboxamide. (Continued)

519	22.39	0.29	-	-	δCC(27), υCCl(16), δC=O(27)
486	3.02	0.04	486	-	γCCl(33), τPz(31), γCC(19)
443	10.42	3.91	-	-	υCCl(39), δCN(12)
437	4.07	0.60	438	-	τPh(56), γCCl(26)
408	11.33	0.13	410	412	τPz(85)
405	3.18	3.68	-	-	δCCl(36), δCN(16)
375	16.25	6.15	-	380	δCCl(35), δCN(13), δPh(17)
309	3.49	1.92	-	315	δCCl(34), δPz(24), δCC(10)
304	0.01	0.33	-	-	τPh(23), γCC(14), γNH(19), γCCl(18)
261	0.95	2.40	-	266	δCCl(49), δNH(14), δC=O(15)
252	1.52	3.85	-	-	γCC(19), γCCl(24), τPh(23)
197	1.72	0.55	-	195	δNH(16), δCCl(14), δPz(11), δPh(10)
162	7.08	1.58	-	166	δCN(30), δCC(23), δCCl(29)
160	0.03	2.01	-	-	τPh(56), γCCl(14)
92	2.41	1.71	-	-	τC=O(54), τCN(18), τNH(15)
86	1.45	3.89	-	-	τPz(41), τNH(25), τPh(10)
57	0.09	0.24	-	-	τC=O(34), δCC(23), τNH(22)
39	0.54	0.73	-	-	τCN(40), τC=O(26), τNH(22)
28	0.63	1.05	-	-	τNH(46), τCN(25)

[a]υ-stretching; δ-in-plane deformation; γ-out-of-plane deformation; τ-torsion; Ph-phenyl ring; Pz-pyrazine ring; potential energy distribution (%) is given in brackets in the assignment column.

(out of-plane deformation) which are in agreement with literature [34, 25, 40].

The phenyl CH stretching modes are assinged at 3125, 3091, 3063 (IR), 3130, 3090 (Raman) and 3128, 3091, 3077, 3063 cm^{-1} theoretically for the title compound according to literature [37]. For the title compound, the phenyl ring stretching modes are observed at 1588, 1564, 1440 cm^{-1} in the IR spectrum and at 1588, 1565, 1440, 1293 cm^{-1} in the Raman spectrum, which is expected in the region 1250-1601 cm^{-1} [37]. In ortho di-substituion the ring breathing mode has three wavenumber intervals depending on whether both substituents are heavy, or one of them is heavy, while the other is light, or both of them are light. In the first case, the interval is 1100-1130 cm^{-1}, in the second case 1020-1070 cm^{-1} while in the third case it is between 630 and 780 cm^{-1} [37, 42]. The reported values of the ring breathing mode of ortho substituted phenyl ring are 1030 (IR), 1030 (Raman), 1022 cm^{-1} (DFT) [43], 1041 cm^{-1} [44], 1011 cm^{-1} [45], 1020 cm^{-1} [46], 1022, 1027 cm^{-1} [47]. For the title compound the ring stretching mode is assinged at 1024 cm^{-1} in IR, 1030 cm^{-1} in Raman and at 1026 cm^{-1} theoretically [37, 42]. The CH deformations of the phenyl ring are expected above 1000 cm^{-1} (in-plane bending modes) and below 1000 cm^{-1} (out-of-plane bending modes [37] and in the present case these modes are assigned at 1261, 1104 (IR), 1260 (Raman), 1260, 1127, 1100, 1009 cm^{-1} (DFT) (in-plane bending modes) and at 972, 926, 853 (IR), 850 (Raman), 970, 929, 855, 743 cm^{-1} (DFT) (out-of-plane bending modes). The ring deformation modes are also identified and assigned Table 2) and most of the modes are not pure but contains significant contributions from other modes also. The root mean square value between the calculated and observed wavenumbers were calculated inorder to investigate the performance of the vibrational wavenumbers of the title compound and the RMS errors are 5.32 for IR bands and 6.42 for Raman bands.

3.3. Nonlinear optical properties

The computational approach allows the determination of nonlinear optical properties as an in expensive way to design molecules by analyzing their potential before synthesis and to determine the hyperpolarazibility values [48]. The polarizability values represent the nonlinear contribution to the induced dipole moment and are noteworth because of their fundamental role in the interpreation of the nonlinear properties in the molecular systems [49]. Many organic molecules, containing conjugated π electrons characterized by large values of hyperpolarizabilites were analyzed by means of vibrational spectroscopy [50]. The calculated values of the dipole moment and polarazibility are 1.864 Debye and 7.728×10^{-23} esu. The first order hyperpolarizability of the title compound is calculated and is found to be 10.15×10^{-30} esu which is comparable with the reported values of similar derivatives [25, 40]. The calculated hyperpolarizability of the title compound is 78.08 times that of the standard NLO material urea (0.13×10^{-30}esu) [51]. The theoretical second order hyperpolarizability was calculated using the Gaussian09 software and is equal to -15.04×10^{-37}e.s.u. We conclude that the title compound and its derivatives are an attractive object for future studies of nonlinear optical properties. For the title compound, the calculated C-N distances in the molecular structure are intermediate between those of C-N single and C=N double bond and therefore, the calculated data suggest an extended π-electron delocalization of the pyrazine ring and carboxamide moiety [52] which is reponsible for the nonlinearity of the molecule.

3.4. Frontier molecular orbitals

Molecular orbital and their properties, like energy are very useful for predicting the most reactive position in π-electron systems and also explained several types of reaction in conjugated systems [53]. The HOMO-LUMO energy gap has been used to prove the bioactivity from the intermolecular charge transfer [54]. The HOMO-LUMO energy gap shows that the energy gap reflects the chemical reactivity and the level of conductivity of the molecule [55]. Smaller the value of energy gap, the easier electron transfer occurs from HOMO to LUMO. Relatively large gap means the molecule would not be kinetically stable [56]. In the present case the energy values of HOMO and LUMO are -7.827 and -

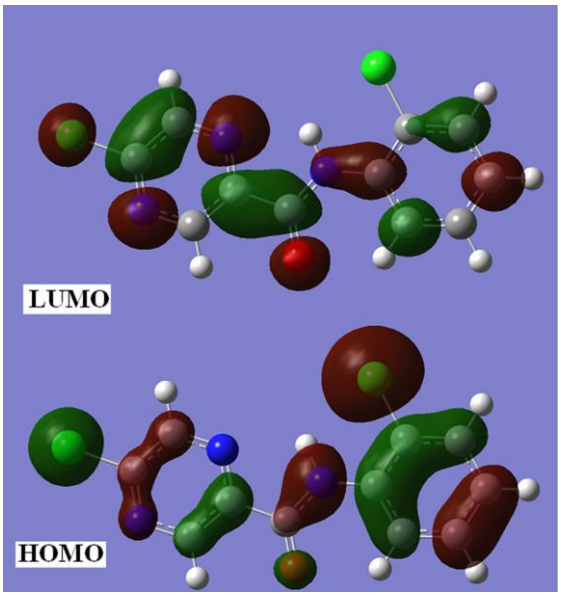

Figure 4. HOMO-LUMO plots of 5-chloro-N-(2-chlorophenyl) pyrazine-2-carboxamide.

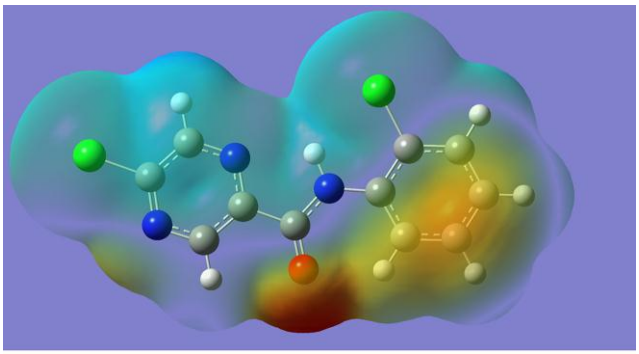

Figure 5. MEP plot of 5-chloro-N-(2-chlorophenyl)pyrazine-2-carboxamide.

4.845 eV, respectively. The ionization energy and electron affinity can be expressed as: $I = -E_{HOMO}$ and $A = -E_{LUMO}$: I = 7.827 and A = 4.845 eV. The differenct global descriptors are given by, hardness $\eta = (I-A)/2$, chemical potential $\mu = -(I+A)/2$ and electrophilicity index $\omega = \mu^2/2\eta$ [57, 58]. In the present case the values of these descriptors are η= 1.491, μ = -6.336 and ω = 13.46 and the energy gap between HOMO and LUMO orbitals is 2.982 eV. Figure 4 shows the distributions of the HOMO and LUMO orbitals and the HOMO is localized over the entire molecule while the LUMO is over the entire molecule, except the chlorine atom attached with the phenyl ring. Both the HOMO and LUMO are mainly localized on the pyrazine ring, indicating that the HOMO-LUMO are mostly the π-anti-bonding type orbital.

3.5. Molecular electrostatic potential

The molecular electrostatic potential has been used for predicting sites and relative reactivities towards electrophilic attack, in studies of biological recognition and hydrogen bonding interactions [59]. The molecular electrostatic potential provides a visual method to understand the relative polarity of a molecule and such surfaces depict the size, shape, charge density and site of chemical reactivity of the molecule. In the MEP surface generated, negative potential corresponds to an attraction of the proton by the concentrated electron density in the molecules (colored as red) and positive electrostatic potential corresponds to repulsion of the proton by the atomic nuclei in regions where low electron density exists and the nuclear charge is incompletely shielded (colored in shades of blue). The electrostatic potential increases in the order red < orange < yellow < green < blue. As seen from the Figure 5, the regions of negative potential are C=O and phenyl ring where the positive potential regions are other parts of the title molecule.

3.6. Natural bond orbital analysis

The natural bond orbitals (NBO) calculations were performed using NBO 3.1 program [60] at the DFT/B3LYP level in order to understand various second-order interactions and the important results given in Tables 3 and 4. The various strong intra-molecular hyper conjugative interactions are: C_4-C_5 from Cl_{11} of $n_3(Cl_{11})\rightarrow\pi^*(C_4\text{-}C_5)$, C_{21}-O_{22} from N_{12} of $n_1(N_{12})\rightarrow\pi^*(C_{21}\text{-}O_{22})$, C_{13}-C_{14} from N_{15} of $n_1(N_{15})\rightarrow\sigma^*(C_{13}\text{-}C_{14})$, C_{18}-C_{19} from N_{16} of $n_1(N_{16})\rightarrow\pi^*(C_{18}\text{-}C_{19})$, C_{21}-N_{12} from O_{22} of $n_2(O_{22})\rightarrow\sigma^*(C_{21}\text{-}N_{12})$ and C_{19}-N_{16} from Cl_{24} of $n_3(Cl_{24})\rightarrow\pi^*(C_{19}\text{-}N_{16})$ with electron densities, 0.38721, 0.33232, 0.03641, 0.04401, 0.06812, 0.39706e and stabilization energies, 8.43, 69.34, 9.13, 10.04, 22.98, 13.28 KJ/mol. The natural hybrid orbitals with higher energy orbitals and 100% p-character are: $n_3(Cl_{11})$, $n_2(O_{22})$, $n_3(Cl_{24})$ with energies, -0.32753, -0.26062, -0.33242a.u and with low occupation numbers, 1.95067, 1.87423, 1.92203. The orbitals with lower energy values are: $n_1(Cl_{11})$, $n_1(O_{22})$, $n_1(Cl_{24})$ having a lower energy value, -0.92376, -0.70490, -0.92203a.u with p-characters, 15.77, 38.16, 15.02% and high occupation numbers, 1.99419, 1.97655, 1.99478. Thus, a very close to pure p-type lone pair orbital participates in the electron donation to the $\pi^*(C_4\text{-}C_5)$ orbital for $n_3(Cl_{11})\rightarrow\pi^*(C_4\text{-}C_5)$, $\pi^*(C_{21}\text{-}O_{22})$ orbital for $n_1(N_{12})\rightarrow\pi^*(C_{21}\text{-}O_{22})$, $\sigma^*(C_{13}\text{-}C_{14})$ orbital for $n_1(N_{15})\rightarrow\sigma^*(C_{13}\text{-}C_{14})$, $\sigma^*(C_{18}\text{-}C_{19})$ orbital for $n_1(N_{16})\rightarrow\sigma^*(C_{18}\text{-}C_{19})$, $\sigma^*(C_{21}\text{-}N_{12})$ orbital for $n_2(O_{22})\rightarrow\sigma^*(C_{21}\text{-}N_{12})$ and $\pi^*(N_{16}\text{-}C_{19})$ orbital for $n_3(Cl_{24})\rightarrow\pi^*(N_{16}\text{-}C_{19})$ interaction in the compound.

3.7. Antiviral activity

In vitro activity of 5-chloro-*N*-(2-chlorophenyl)pyrazine-2-carboxamide was determined against a broad panel of various clinically important DNA and RNA viruses. The virus panel (see experimental section for the full list) included pathogens of medical importance such as herpesviruses, respiratory syncytial virus (RSV), HIV and influenza virus. No antiviral activity was detected up to the highest tested concentration, which was (due to limited solubility in the testing medium) 20 µM for most of the viruses, 25 µM for HIV, and 100 µM for influenza viruses.

3.8. Molecular docking

The enzyme glucosamine 6-phosphate deaminase (GlcN6P deaminase,) catalyzes the reversible isomerization and deamination of D-glucosamine 6-phosphate (GlcN6P) into D-fructose 6-phosphate and ammonium ion [61]. Glucosamine-6-phosphate synthase is the only member of the amidotransferase subfamily of enzymes. The molecular mechanism of reaction catalysed by GlcN-6-P synthase is complex and involves both amino transfer and sugar isomerisation. GlcN-6-P synthase is inflicted in phenomenon of hexosamine induced insulin resistance in diabetes [62]. Pyrazine and their derivatives in the past decade and were found to possess promising antitumor, anticonvulsant, antimicrobial, anti-tubercular and anti-diabetic activities [63]. High resolution crystal structure of glucosamine 6-phosphate deaminase was downloaded from the RSCB protein data bank website with PDB ID: 1FQO. All molecular docking calculations were performed on Auto Dock-Vina software [64]. The 3D crystal structure of glucosamine 6-phosphate deaminase was obtained from Protein Data Bank and the protein was prepared for docking by removing the co-crystallized ligands, waters and co-factors. The Auto Dock Tools (ADT) graphical user interface was used to calculate Kollman charges and polar hydrogens. The ligand was prepared for docking by minimizing its energy at B3LYP/6-31G (6D, 7F) level of

Table 3. Second order perturbation theory analysis of Fock matrix in NBO basis corresponding to the intra-molecular bonds of the title compound.

Donor(i)	Type	ED/e	Acceptor(j)	Type	ED/e	E(2)[a]	E(j)-E(i)[b]	F(i,j)[c]
C1-C6	σ	1.972	C1-C2	σ*	0.015	2.15	1.28	0.047
			C4-C5	σ*	0.021	3.14	1.26	0.056
			C5-Cl11	σ*	0.036	5.27	0.78	0.057
C4-C5	σ	1.980	C3-C4	σ*	0.016	2.49	1.30	0.051
			C5-C6	σ*	0.031	4.15	1.27	0.065
			C6-N12	σ*	0.028	3.45	1.15	0.056
	π	1.715	C1-C6	π*	0.387	18.97	0.30	0.069
			C2-C3	π*	0.338	15.99	0.31	0.063
C5-C6	σ	1.978	C1-C6	σ*	0.022	3.30	1.28	0.058
			C4-C5	σ*	0.021	3.51	1.30	0.060
			C6-N12	σ*	0.028	1.55	1.15	0.038
			N12-C21	σ*	0.068	2.78	1.20	0.052
N12-C21	σ	1.989	C5-C6	σ*	0.031	1.83	1.38	0.045
			C6-N12	σ*	0.028	2.08	1.26	0.046
			C13-C14	σ*	0.036	1.51	1.37	0.041
C13-C14	σ	1.987	N12-C21	σ*	0.068	1.78	1.21	0.042
			C13-N15	σ*	0.023	1.45	1.23	0.038
			C13-C21	σ*	0.070	2.09	1.15	0.044
C13-C21	σ	1.975	C6-N12	σ*	0.028	4.21	1.10	0.061
			C13-C14	σ*	0.036	1.44	1.21	0.037
			C13-N15	σ*	0.023	1.08	1.16	0.032
			C14-N16	σ*	0.014	2.51	1.17	0.049
			N15-C18	σ*	0.016	3.07	1.18	0.054
N16-C19	σ	1.989	C18-C19	σ*	0.044	1.87	1.40	0.046
	π	1.718	C13-C14	π*	0.292	21.09	0.34	0.076
			N15-C18	π*	0.336	17.46	0.31	0.067
C18-C19	σ	1.992	N16-C19	σ*	0.028	1.60	1.28	0.041
C19-Cl24	σ	1.987	C14-N16	σ*	0.014	3.29	1.17	0.055
			N15-C18	σ*	0.016	2.83	1.18	0.052
C21-O22	π	1.973	C13-C14	π*	0.292	4.09	0.36	0.037
LPCl11	σ	1.994	C5-C6	σ*	0.031	1.20	1.45	0.037
	π	1.967	C4-C5	σ*	0.021	2.87	0.90	0.045
			C5-C6	σ*	0.031	2.86	0.86	0.044
	n	1.951	C4-C5	π*	0.387	8.43	0.34	0.052
LPN12	σ	1.627	C1-C6	π*	0.387	36.08	0.29	0.092
			C21-O22	π*	0.332	69.34	0.26	0.121
LPN15	σ	1.912	C13-C14	σ*	0.036	9.13	0.92	0.083
			C13-C21	σ*	0.070	2.44	0.79	0.039
			C18-C19	σ*	0.044	9.02	0.89	0.081
LPN16	σ	1.901	C13-C14	σ*	0.036	8.75	0.90	0.081
			C18-C19	σ*	0.044	10.04	0.88	0.085
			C19-Cl24	σ*	0.074	5.23	0.45	0.044
LPO22	σ	1.977	N12-C21	σ*	0.068	2.35	1.16	0.047
			C13-C21	σ*	0.070	2.03	1.10	0.043
	π	1.874	N12-C21	σ*	0.068	22.98	0.72	0.116
			C13-C21	σ*	0.070	18.45	0.66	0.100
LPCl24	σ	1.995	C18-C19	σ*	0.044	1.13	1.43	0.036
	π	1.971	N16-C19	σ*	0.028	5.05	0.83	0.058
			C18-C19	σ*	0.044	3.07	0.83	0.045
	n	1.922	N16-C19	π*	0.397	13.28	0.29	0.060

[a]E(2) means energy of hyper-conjugative interactions (stabilization energy in kJ/mol)
[b]Energy difference (a.u.) between donor and acceptor i and j NBO orbitals
[c]F(i,j) is the Fock matrix elements (a..u) between i and j NBO orbitals

Table 4. NBO results showing the formation of Lewis and non-Lewis orbitals.

Bond(A-B)	ED/e[a]	EDA%	EDB%	NBO	s%	p%
σ C1-C6	1.966 -0.705	47.95	52.05	0.6925($sp^{2.03}$)C+ 0.7214($sp^{1.70}$)C	32.93 37.06	67.07 62.94
σ C4-C5	1.980 -0.740	49.09	50.91	0.7007($sp^{1.91}$)C+ 0.7135($sp^{1.45}$)C	34.32 40.76	65.68 59.24
π C4-C5	1.715 -0.280	45.78	54.22	0.6766($sp^{1.00}$)C+ 0.7363($sp^{1.00}$)C	0.00 0.00	100.0 100.0
σ C5-C6	1.978 -0.739	49.49	50.91	0.7035($sp^{1.57}$)C+ 0.7170($sp^{1.86}$)C	38.92 34.98	61.08 65.02
σ N12-C21	1.989 -0.848	62.80	37.20	0.7925($sp^{1.80}$)N+ 0.6099($sp^{2.08}$)C	35.64 32.40	64.36 67.60
σ C13-C14	1.987 -0.756	51.33	48.67	0.7164($sp^{1.68}$)C+ 0.6976($sp^{1.73}$)C	37.26 36.59	62.74 63.41
σ C13-C21	1.975 -0.691	52.18	47.82	0.7224($sp^{2.05}$)C+ 0.6915($sp^{1.85}$)C	32.79 35.04	67.21 64.96
σ N16-C19	1.989 -0.902	59.15	40.85	0.7691($sp^{1.71}$)N+ 0.6391($sp^{1.90}$)C	36.78 34.52	63.22 65.48
π N16-C19	1.718 -0.352	55.19	44.81	0.7429($sp^{1.00}$)N+ 0.6694($sp^{1.00}$)C	0.00 0.00	100.0 100.0
σC18-C19	1.992 -0.780	49.25	50.75	0.7018($sp^{1.76}$)C+ 0.7124($sp^{1.38}$)C	36.18 42.03	63.82 57.97
σC19-Cl24	1.987 -0.693	45.58	54.42	0.6751($sp^{3.27}$)C+ 0.7377($sp^{5.57}$)Cl	23.39 15.15	76.61 84.85
πC21-O22	1.973 -0.370	30.39	69.61	0.5512($sp^{1.00}$)C+ 0.8343($sp^{1.00}$)O	0.00 0.00	100.0 100.0
n1Cl11	1.994 -0.924	-	-	$sp^{0.19}$	84.23	15.77
n2Cl11	1.967 -0.334	-	-	$sp^{99.99}$	0.56	99.44
n3Cl11	1.951 -0.328	-	-	$sp^{1.00}$	0.00	100.0
n1N12	1.627 -0.273	-	-	$sp^{1.00}$	0.00	100.0
n1N15	1.912 -0.393	-	-	$sp^{2.48}$	28.68	71.32
n1N16	1.901 -0.380	-	-	$sp^{2.51}$	28.43	71.57
n1O22	1.977 -0.705	-	-	$sp^{0.62}$	61.84	38.16
n2O22	1.874 -0.261	-	-	$sp^{1.00}$	0.00	100.0
n1Cl24	1.995 -0.931	-	-	$sp^{0.18}$	84.98	15.02
n2Cl24	1.971 -0.333	-	-	$sp^{99.99}$	0.09	99.91
n3Cl24	1.922 -0.332	-	-	$sp^{1.00}$	0.00	100.0

[a]ED/e in a.u.

Table 5. The binding affinity values of different poses of the title compound predicted by Autodock Vina.

Mode	Affinity (kcal/mol)	Distance from best mode (Å)	
		RMSD l.b.	RMSD u.b.
1	-6.4	0.000	0.000
2	-6.3	16.000	17.494
3	-5.9	15.604	16.062
4	-5.9	15.517	16.703
5	-5.5	15.509	16.908
6	-5.4	15.629	16.383
7	-54.	25.660	24.969
8	-5.3	21.630	22.584
9	-5.2	25.087	26.492

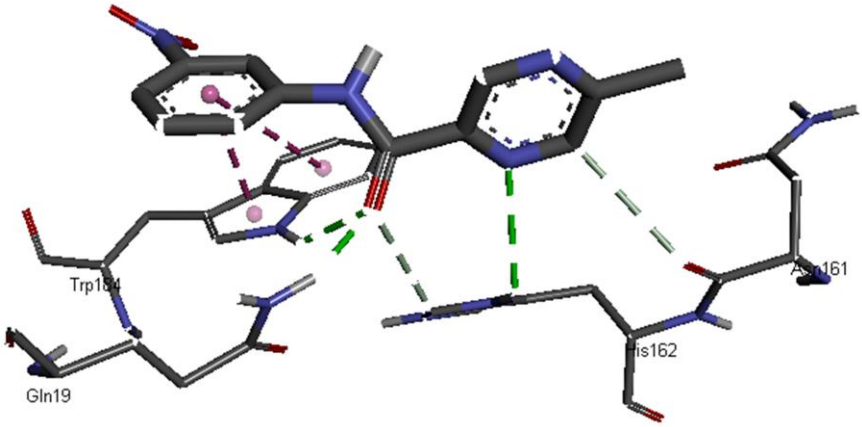

Figure 6. Schematic for the ligand interaction with the active site of glucosamine-6-phosphate deaminase.

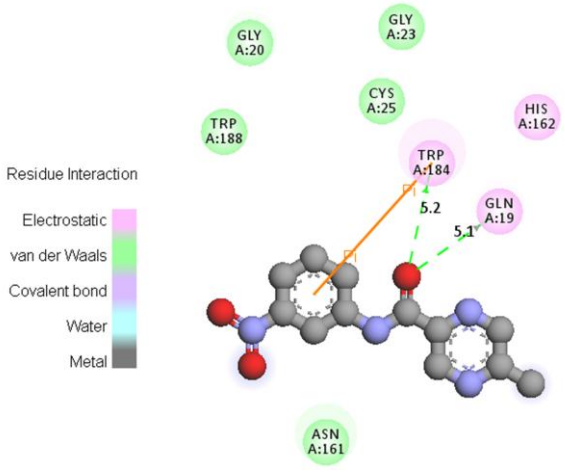

Figure 7. 2D interactive plot of ligand and glucosamine-6-phosphate deaminase receptor.

theory and partial charges were calculated by Geistenger method. The active site of the enzyme was defined to include residues of the active site within the grid size of 40Å×40Å×40Å. The most popular algorithm, Lamarckian Genetic Algorithm (LGA) available in Autodock was employed for docking. The docking protocol was tested by extracting co-crystallized inhibitor from the protein and then docking the same. The docking protocol predicted the same conformation as was present in the crystal structure with RMSD value well within the reliable range of 2Å [65]. Amongst the docked conformations, one which binds well at the active site was analysed for detailed interactions in Discover Studio Visualizer 4.0 software. The ligand binds at the active site of the substrate (Figures 6 and 7) by weak non-covalent interactions. Amino acid Leu106 forms H-bond with the docked ligand. The docked ligand title compound forms a stable complex with glucosamine 6-phosphate deaminase and gives a binding affinity (ΔG in kcal/mol) value of -6.4 (Table 5). These preliminary results suggest that the compound might exhibit inhibitory activity against glucosamine 6-phosphate deaminase (Figure 8).

4. CONCLUSIONS

The FT-IR and FT-Raman spectra of the title compound were reported experimentally and theoretically. The HOMO and LUMO analysis are used to determine the charge transfer within the molecule. The chemical reactivity is understood from the chemical potential, electrophilicity and global hardness. The stability of the molecule arising from hyeprconjugative interaction and charge delocalization has been analyzed using natural bond orbital analysis. MEP predicts the most reactive part in the molecule. Optimized geometrical parameters of the title compound are in agreement with that of similar derivatives. The hyperpolarizability values of the title compound are also determined and from the study reveals that the title compound and its derivatives are attractive objects for future studies in nonlinear optics. The title compound binds at the active site of the substrate by weak non-covalent interactions and the amino acid Leu106 forms H-bond with the docked

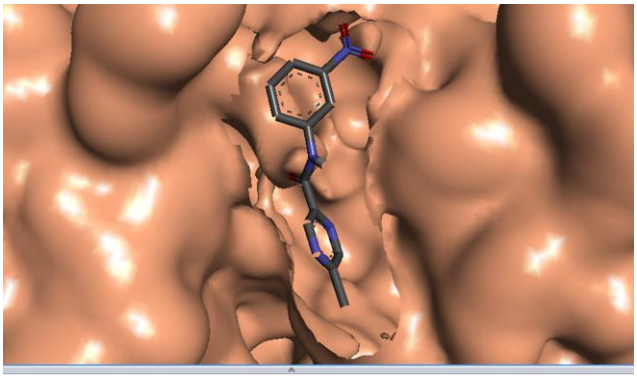

Figure 8. Pictorial representation with docked ligand embedded in the active site of glucosamine-6-phosphate deaminase.

ligand. As an additional test, in vitro antiviral activity of the title compound was evaluated against broad panel of clinically important viruses. No antiviral activity was detected in the tested concentrations.

ACKNOWLEDGEMENTS

Authors wish to thank Associate Professor Lieve Naesens (Rega Institute for Medical Research, Laboratory of Virology and Chemotherapy, Leuven, Belgium) for coordination of antiviral testing. The authors would like to extend their sincere appreciation to the Deanship of Scientific Research at King Saud University for funding this work through the Research Group Project No. PRG-1436-23.

REFERENCES

1. G. B. Barlin, The Pyrazines: The Chemistry of Heterocyclic Compounds - A series of monographs, John Wiley and Sons, New York (1982).
2. M. R. Robert, Appl. Microbiol. Biotechnol. 85 (2010) 1315.
3. T. B. Adams, J. Doull, V. J. Feron, J. I. Goodman, L. J. Marnett, I. C. Munro, P. M. Newberne, P. S. Portoghese, R. L. Smith, W. J. Waddell, B. M. Wagner, Food Chem. Toxicol. 40 (2002) 429.
4. H. C. Beck, A. M. Hansen, F. R. Lauritsen, FEMS Microbiol. Lett. 220 (2003) 67.
5. R. Wagner, M. Czerny, J. Bielohradsky, W. Grosch, Z Lebensm Unters Forsch A 208 (1999) 308.
6. A. Woolfson, M. Rothschild, Proc. R Soc. Lond. B 242 (1990) 113.
7. J. A. Maga, Food Rev. Int. 8 (1992) 479.
8. T. Yamaguchi, S. Ito, N. Kashige, K. Nakahara, K. Harano, Chem. Pharm. Bull. 55 (2007) 532.
9. J. Zitko, B. Servusova, P. Paterova, J. Mandikova, V. Kubicek, R. Kucera, V. Hrabcova, J. Kunes, O. Soukup, M. Dolezal, Molecules 18 (2013) 14807.
10. Y. Furuta, K. Takahashi, Y. Fukuda, M. Kuno, T. Kamiyama, K. Kozaki, N. Nomura, H. Egawa, S. Minami, Y. Watanabe, H. Narita, K. Shiraki, Antimicrob. Agents Chemother. 46 (2002) 977.
11. R. W. Sidwell, D. L. Barnard, C. W. Day, D. F. Smee, K. W. Bailey, M. H. Wong, J. D. Morrey, Y. Furuta, Antimicrob. Agents Chemother. 51 (2007) 845.
12. Y. Furuta, K. Takahashi, M. Maekawa, H. Maegawa, H. Egawa, N. Terashima, Antimicrob. Agents Chemother. 48 (2004) 199.
13. Y. Furuta, K. Takahashi, K. Shiraki, K. Sakamoto, D. F. Smee, D. L. Barnard, B. B. Gowen, J. G. Julander, J. D. Morrey, Antiviral Res. 82 (2009) 95.
14. J. G. Julander, K. Shafer, D. F. Smee, J. D. Morrey, Y. Furuta, Antimicrob. Agents Chemother. 53 (2009) 202.
15. J. G. Julander, Y. Furuta, K. Shafer, R. W. Sidwell, Antimicrob. Agents Chemother. 51 (2007) 1962.
16. B. B. Gowen, M. H. Wong, K. H. Jung, D. F. Smee, J. D. Morrey, Y. Furuta, Antiviral Res. 86 (2010) 121.
17. B. Servusova, J. Vobickova, P. Paterova, V. Kubicek, J. Kunes, M. Dolezal, J. Zitko, Bioorg. Med. Chem. Lett. 23 (2013) 3589.
18. M. J. Frisch, G. W. Trucks, H. B. Schlegel, G. E. Scuseria, M. A. Robb, J. R. Cheeseman, G. Scalmani, V. Barone, B. Mennucci, G. A. Petersson, H. Nakatsuji, M. Caricato, X. Li, H. P. Hratchian, A. F. Izmaylov, J. Bloino, G. Zheng, J. L. Sonnenberg, M. Hada, M. Ehara, K. Toyota, R. Fukuda, J. Hasegawa, M. Ishida, T. Nakajima, Y. Honda, O. Kitao, H. Nakai, T. Vreven, J. A. Montgomery, Jr., J. E. Peralta, F. Ogliaro, M. Bearpark, J. J. Heyd, E. Brothers, K. N. Kudin, V. N. Staroverov, T. Keith, R. Kobayashi, J. Normand, K. Raghavachari, A. Rendell, J. C. Burant, S. S. Iyengar, J. Tomasi, M. Cossi, N. Rega, J. M. Millam, M. Klene, J. E. Knox, J. B. Cross, V. Bakken, C. Adamo, J. Jaramillo, R. Gomperts, R. E. Stratmann, O. Yazyev, A. J. Austin, R. Cammi, C. Pomelli, J W. Ochterski, R. L. Martin, K. Morokuma, V. G. Zakrzewski, G. A. Voth, P. Salvador, J. J. Dannenberg, S. Dapprich, A. D. Daniels, O. Farkas, J. B. Foresman, J. V. Ortiz, J. Cioslowski, D. J. Fox, Gaussian 09 (Revision B. 01), Gaussian, Inc., Wallingford CT (2010).
19. A. D. Becke, Phys. Rev. 38A (1988) 3098.
20. J. B. Foresman, Exploring Chemistry with Electronic Structure Methods: A Guide to Using Gaussian, Gaussian Inc., Pittsburg, PA (1996).
21. R. Dennington, T. Keith, J. Millam, Gaussview (Version 5), Semichem Inc., (2009).
22. J. M. L. Martin, C. Van Alsenoy, GAR2PED, A Program to Obtain a Potential Energy Distribution from a Gaussian Archive Record, Universit of Antwerp, Belgium (2007).
23. K. Tamagawa, T. Iijima, M. Kimura, J. Mol. Struct. 30 (1976) 243.
24. K. B. Borisenko, C. W. Bock, I. Hargittai, J. Phys. Chem. 100 (1996) 7426.
25. J. Lukose, C. Y. Panicker, P. S. Nayak, B. Narayana, B. K. Sarojini, C. Van Alsenoy, A. A. Al-Saadi, Spectrochim. Acta 135 (2015) 608.
26. V. Chis, A. Piranau, T. Jurca, M. Vasilescu, S. Simon, O. Cozar, L. David, Chem. Phys. 316 (2005) 153.
27. S. M. Bakalova, A. G. Santos, I. Timcheva, J. Kaneti, I. L. Filipova, G. M. Dobrikov, V. D. Dimitrov, J. Mol. Struct. Theochem 710 (2004) 229.
28. J. C. Noveron, A. M. Arif, P. J. Stang, Chem. Mater. 15 (2003) 372.
29. H. Takeuchi, M. Sato, T. Tsuji, H. Takashima, T. Egawa, S. Konaka, J. Mol. Struct. 485-486 (1999) 175.
30. E. D. Stevens, Acta Cryst. 34B (1978) 544.
31. Q. Gao, G. A. Jeffrey, J. R. Ruble, R. K. McMullan, Acta Cryst. 47B (1991) 742.
32. M. Barthes, G. De Nunzio, M. Ribet, Synth. Met. 76 (1996) 337.
33. P. Pazdera, H. Divisova, H. Havilsova, P. Borek, Molecules 5 (2000) 189.
34. G. Socrates, Infrared Characteristic Group Frequencies, John Wiley and Sons, New York (1981).
35. Y. S. Mary, K. Raju, I. Yildiz, O. T. Arpaci, H. I. S. Nogueira, C. M. Granadeiro, C. Van Alsenoy, Spectrochim. Acta 96 (2012) 617.
36. Y. S. Mary, K. Raju, C. Y. Panicker, A. A. Al-Saadi, T. Thiemann, Spectrochim. Acta 131 (2014) 471.
37. N. P. G. Roeges, A Guide to the Complete Interpretaton of Infrared Spectra of Organic Structures, John Wiley and Sons Inc., New York (1994).
38. N. B. Colthup, L. H. Daly, S. E. Wiberly, Introduction of Infrared and Raman Spectroscopy, Academic Press, New York (1975).
39. Y. S. Mary, H. T. Varghese, C. Y. Panicker, M. Dolezal, Spectrochim. Acta 71 (2008) 725.
40. T. Joseph, H. T. Varghese, C. Y. Panicker, K. Viswathan, M. Dolezal, T. K. Manojukumar, C. Van Alsenoy, Spectrochim. Acta 113 (2013) 203.
41. H. Endredi, F. Billes, S. Holly, J. Mol. Struct. Theochem 633 (2003) 73.
42. G. Varsanyi, Assignments of Vibrational Spectra of Seven Hundred Benzene Derivatives, Wiley, New York (1974).
43. R. T. Ulahannan, C. Y. Panicker, H. T. Varghese, R. Musiol, J. Jampilek, C. Van Alsenoy, J. A. War, A. A. Al-Saadi, Spectrochim. Acta 151 (2015) 335.
44. A. Chandran, H. T. Varghese, C. Y. Panicker, C. Van Alsenoy, G. Rajendran, J. Mol. Struct. 1001 (2011) 29.
45. C. Y. Panicker, H. T. Varghese, K. R. Ambujakshan, S. Mathew, S. Ganguli, A. K. Nanda, C. Van Alsenoy, Y. S. Mary, Euro. J. Chem. 1 (2010) 37.
46. C. Y. Panicker, H. T. Varghse, K. R. Ambujakshan, S. Mathew, S. Ganguli, A. K. Nanda, C. Van Alsenoy, Y. S. Mary, J. Mol. Struct. 963 (2010) 137.
47. E. Fazal, C. Y. Panicker, H. T. Varghese, S. Nagarajan, B. S. Sudha, J. A. War, S. K. Srivastava, B. Harikumar, P. L. Anto, Spectrochim. Acta 143 (2015) 213.
48. A. D. McLean, M. Yoshimine, J. Chem. Phys. 47 (1967) 1927.
49. N. Bloembergen, Non-linear Optics, Benjamin Inc., New York (1965).
50. C. Castiglioni, M. Del Zoppo, P. Zuliani, G. Zerbi, Synth. Met. 74 (1995) 171.
51. M. Adant, M. Dupuis, J. L. Bredas, Int. J. Quantum Chem. 56 (2004) 497.
52. Y. P. Tian, W. T. Yu, C. Y. Zhao, M. H. Jiang, Z. G. Cari, H. K. Fun, Polyhedron 21 (2002) 1217.
53. K. Fukui, I. Yonezawa, H. Shingu, J. Chem. Phys. 20 (1952) 722.

54. L. Padmaja, C. Ravikumar, D. Sajan, I. H. Joe, V. S. Jayakumar, GR. Pettit, O. F. Nielsen, J. Raman Spectrosc. 40 (2009) 419.
55. B. Kosar, C. Albayrak, Spectrochim. Acta 78 (2011) 160.
56. T. E. Rosso, M. W. Elzy, J. O. Jensen, H. F. Hameka, D. Zeroka, Spectrochim. Acta 55 (1998) 121.
57. R. J. Parr, L. V. Szentpaly, S. Liu, J. Am. Chem. Soc. 121 (1999) 1922.
58. R. J. Parr, R. G. Pearson, J. Am. Chem. Soc. 105 (1983) 7512.
59. J. S. Murray, K. Sen, Molecular Electrostatic Potentials, concepts and applications, Elsevier, Amsterdam (1996).
60. E. D. Glendening, A. E. Reed, J. E. Carpenter, F. Weinhold, NBO (Version 3. 1), University of Wisconsin, Madison (1998).
61. G. Oliva, M. R. M. Fontes, R. C. Garratt, M. M. Altamirano, M. L. Calcagno, E. Horjales, Structure 3 (1995) 1323.
62. S. Milewski, Biochim. Biophys. Acta 1597 (2002) 173.
63. C. P. Meher, A. M. Rao, M. Omar, Asian J. Pharm. Sci. Res 3 (2013) 43.
64. O. Trott, A. J. Olson, J. Comput. Chem. 31 (2010) 455.
65. B. Kramer, M. Rarey, T. Lengauer, Proteins: Struct. Funct. Genet. 37 (1999) 228.

Cite this article as:

S. H. Rosline Sebastian *et al.*: Synthesis, spectroscopic investigations, quantum chemical studies, molecular docking and antiviral activity of 5-chloro-N-(2-chlorophenyl)pyrazine-2-carboxamide. Sci. Adv. Today 2 (2016) 25239.